LATTICE COMPENSATION OF THE WIGGLER EFFECT IN HLSII WITH PARTICLE SWARM OPTIMIZATION*

Gangwen Liu, Ke Xuan†, Lin Wang
National Synchrotron Radiation Laboratory,
University of Science and Technology of China, Hefei, Anhui 230029, China

Abstract

The upgrade project of Hefei Light Source (HLSII) has successfully reduced the natural emittance of the electron beam to lower than 40 nm·rad at 800 MeV with five insertion devices installed. To provide enough straight sections for these insertion devices, the lattice structure has been changed to four double bend achromatic (DBA) with two super-periods from the former four triple bend achromatic (TBA). These different types of the insertion devices can greatly improve the performance of the light source, but simultaneously they can also influence the dynamics of the electron beam in the storage ring. Especially they can bring the distortion of the linear beam optics seriously. In order to make sure the stability and the quality of the beam meeting the design goal, the effect of these insertion devices must be compensated. In this paper, a direct compensation method is applied for the wiggler in the HLSII storage ring with the particle swarm optimization.

INTRODUCTION

The Hefei Light Source (HLS) was a second generation synchrotron radiation light source, which had been operated for over two decades in the VUV to soft X-ray range with natural emittance of 166 nm·rad at electron beam energy of 800 MeV. To better satisfy the increasing requirements of synchrotron radiation experiments, an upgrade project of HLS to enhance its performance, named HLSII, was proposed and then launched in July, 2010.

The philosophy for the design of the HLSII storage ring is to reduce the natural emittance of electron beam and increase the number of straight sections for insertion devices while maintaining the former foundation. Following this philosophy, the new storage ring lattice was designed [1] and studied [2, 3]. The circumference of the new storage ring remains 66.1308 m. Strong focusing quadrupoles are employed to obtain lower natural emittance of less than 40 nm·rad at the nominal energy of 800 MeV in the achromatic mode. Table 1 shows the main design parameters of the HLSII ring. Its lattice structure is changed to 4×DBA from the former 4×TBA with two super-periods to provide more straight sections for insertion devices. The designed transverse beta functions are shown in Fig. 1. In the new lattice, there are eight straight sections in total applied for beam injection, RF cavity and insertion devices. Five insertion devices have been equipped in the HLS-II storage ring. The periodic magnetic field in these insertion devices leads to tune shift and beta function distortion, which is similar to the focusing effect of the fringe field in dipoles. Therefore the effect of these insertion devices must be compensated carefully to make them transparent to the storage ring.

Table 1: Main Parameters of the HLS-II Storage Ring

Beam energy [MeV]	800
Beam current [mA]	300
Natural emittance [nm·rad]	< 40
Beam lifetime [hours]	> 5
RF Frequency [MHz]	204
Harmonic number	45
Natural energy spread (rms)	0.00047
Slow orbit drifts	< 0.1 σ
Transverse tune	4.4447/2.3597

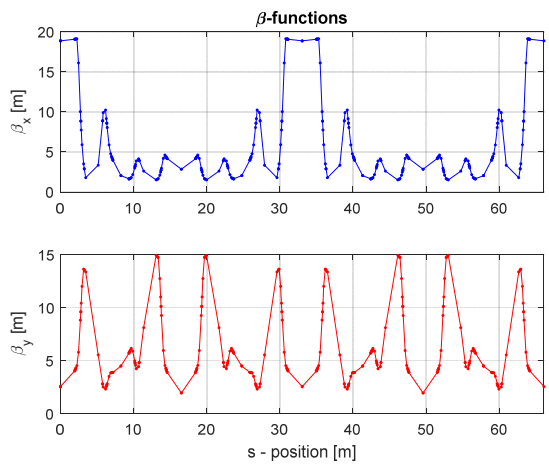

Figure 1: Transverse beta functions of the HLSII storage ring.

In this paper, a direct compensation method using the particle swarm optimization (PSO) with an acurate theoretical model is applied for the compensation of the wiggler effect in the HLSII storage ring.

THEORETICAL MODEL OF WIGGLER

The compensation of the wiggler is the priority due to their serious effect on the beam in the storage ring. In order to analysis the exact effect of the wiggler, a theoretical model of the planar horizontal wiggler is chosen. The canonical integration routines which are programmed by Y. K. Wu [4] have been applied for the compensation.

* Work supported by NSFC (11175182, 11175180)
† xuanke@ustc.edu.cn

ISBN 978-3-95450-147-2

The field expansion used by the code for a horizontally deflecting wiggler is expressed in following form:

$$
\begin{aligned}
B_y &= -B_0 \sum_{m,n} C_{mn} \cos(k_{xl}x)\cosh(k_{ym}y) \\
&\quad \cos(k_{zn}z + \theta_{zn}) \\
B_x &= B_0 \sum_{m,n} C_{mn} \frac{k_{xl}}{k_{ym}} \sin(k_{xl}x)\sinh(k_{ym}y) \\
&\quad \cos(k_{zn}z + \theta_{zn}) \\
B_z &= B_0 \sum_{m,n} C_{mn} \frac{k_{zn}}{k_{ym}} \cos(k_{xl}x)\sinh(k_{ym}y) \\
&\quad \sin(k_{zn}z + \theta_{zn})
\end{aligned}
\qquad (1)
$$

where B_0 is the peak value of the on-axis magnetic field, C_{mn} give the relative amplitudes of wiggler harmonics, θ_{zn} is the relative phase of the nth wiggler harmonic, the wavenumbers satisfy $k_{ym}^2 = k_{xl}^2 + k_{zn}^2$, $k_{zn} = nk_w$ and $k_{ym}^2 k_w = 2\pi/\lambda_w$. λ_w is the wiggler period.

The wiggler installed in HLSII storage ring is a hybrid permanent magnet and also a planar horizontal wiggler. Some of its main parameters are listed in Table 2.

Table 2: Parameters of the Wiggler in HLSII

Period [m]	0.140
Number of periods	12
Total length [m]	1.680
Gap [mm]	30~200
Peak value of the magnetic field [T]	~1.22

With the parameters and the model mentioned above, we can simulate the effect of the wiggler in HLSII storage ring with the accelerator toolbox [5]. The transverse beta functions of the storage ring with the wiggler are plotted in Fig. 2.

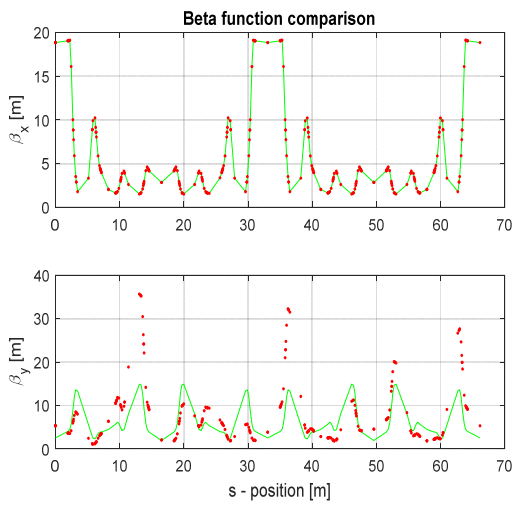

Figure 2: Comparison of the transverse beta function with and without the wiggler.

The green line shows the design values of the transverse beat functions, and the red dots indicate the calculated beta functions with the theoretical model of the wiggler. Compared with their design values, the horizontal beta function and tune are almost the same, but vertical ones are distorted seriously. The vertical beta beating is up to 139.27% at the most with the effect of the wiggler and the vertical tune shift can be as much as 0.079 from the design value 2.3597 to 2.4388. Considering these serious effects on the beam, +the lattice is compensated for with all of quadrupoles in the storage ring.

LATTICE COMPENSATION WITH PSO

Particle Swarm Optimization (PSO) is an Artificial Intelligence algorithm attributed originally to James Kennedy and R.C. Eberhart in 1995 [6] and modified by Yuhui Shi in 1998 [7]. The PSO algorithm was first intended for simulating social behavior, as a stylized representation of the movement of organisms in a bird flock or fish school, and then this simplified algorithm was observed to be performing optimization. Because the algorithm is quite easy to understand and has many advantages in optimization, it has been applied in the beam emittance optimization [8], enlarging dynamic and momentum Aperture [9] and chromaticity compensation [10] in storage rings.

A basic variant of the PSO algorithm works by creating a group of populations which is called a swarm. And each population is composed of candidate solutions which are called particles. Each particle moves around with its own velocity in the search-space according to a few simple formulae. The movement is guided by its own best known position and the best known position of the entire swarm. The equations of the movement for each particle are expressed as follows:

$$
\begin{aligned}
v_{id}(t+1) &= w \cdot v_{id}(t) + c_1 \cdot r_1 \cdot (p_{id}(t) - x_{id}(t)) \\
&\quad + c_2 \cdot r_2 \cdot (p_{gd}(t) - x_{id}(t)) \\
x_{id}(t+1) &= x_{id}(t) + v_{id}(t+1)
\end{aligned}
\qquad (2)
$$

where x_{id}, v_{id}, and p_{id} indicate the position, velocity and best position of the i^{th} particle in the d^{th} dimension respectively, p_{gd} is the global best position of the entire swarm in the d^{th} dimension, w is the inertia weight, c_1 is the cognitive learning factor, c_2 is the social learning factor, and $r_{1,2}$ are two uniformly distributed random variables in the range [0, 1].

The parameters mentioned in Eq. (2) directly decide the convergence speed and the final results. They can be determined by the following equations [11]:

$$
\begin{aligned}
v_{id}(t+1) &= \chi \left\{ \begin{matrix} v_{id}(t) + c_1 \cdot r_1 \cdot (p_{id}(t) - x_{id}(t)) \\ + c_2 \cdot r_2 \cdot (p_{gd}(t) - x_{id}(t)) \end{matrix} \right\} \\
\chi &= \frac{2}{\left| 2 - \varphi - \sqrt{\varphi^2 - 4\varphi} \right|}, \quad \varphi = c_1 + c_2 > 4
\end{aligned}
\qquad (3)
$$

where χ is the constriction factor. When the learning factor c_1 and c_2 are chosen 2.05, the random positive numbers φ will be 4.1 and the constriction factor χ will be 0.729. Therefore the parameters in Eq. (3) can be obtained with $w = 0.729$ and $c_1 = c_2 = 1.49$.

The fitness function is created by the distance between the design beta functions and the calculated ones with the wiggler, which can be described with the formula as follows:

$$\chi^2 = \sum_{j=1}^{N} \left[B_{wiggler}(j) - B_{design}(j) \right]^2 \quad (4)$$

Where $B_{wiggler}$ and B_{design} are beta functions calculated or measured at each quadrupoles. N is the number of the quadrupoles.

The initial population size is 10000, and the iteration limit is set up to 1000. After 673 iterations, the compensated values of these quadrupoles are given by the fitting result. The comparison of the transverse beta functions between the design values and the ones after compensation of the wiggler is shown in Fig. 3.

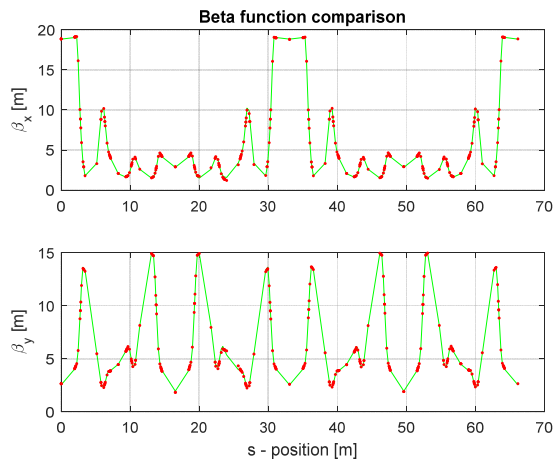

Figure 3: Comparison of the transverse beta functions between the design values and the compensated ones of the wiggler.

The green line shows the design values of the transverse beat functions, and the red dots indicate the calculated beta functions with the theoretical model of the wiggler after the compensation.

We can see that the transverse beta functions have been improved greatly after the compensation. Most of the beta functions calculated in 292 positions along the storage ring are almost the same with the design value expect for the ones at the wiggler position which is about 24 m from the injection point. The maximum beta beating occurs at the side of the wiggler, which is about 50%. The strength change of each quadrupole is presented in Fig. 4. It is clear to see that the strengths of the two quadrupoles Q12 and Q13 around the wiggler have the largest changes, and other quadrupole strengths also have obvious changes. After the global compensation, the transverse tunes are [4.4440, 2.3597] against the theoretical values [4.4447, 2.3598], which are more precise than the ones [4.4447, 2.4388] before the compensation.

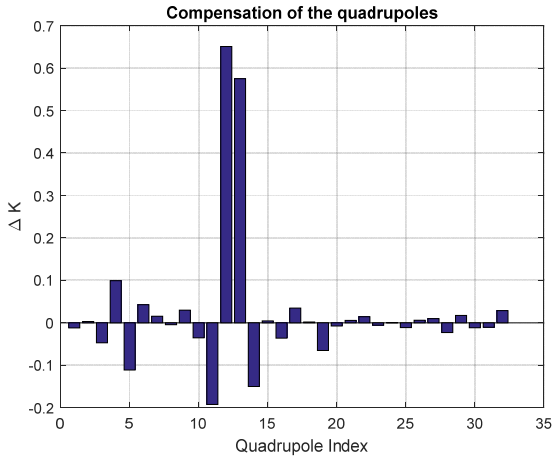

Figure 4: Changes of all the quadrupole strengths after the compensation.

SUMMARY

The insertion devices have become more and more essential for the storage ring to improve the performance of the light source. Therefore the lattice compensation of their effect turns out a necessary work for the operation of the storage ring. In this paper, we first applied the PSO algorithm to compensate the effect of the wiggler. The compensation progress is more direct, and the result shows very good.

REFERENCES

[1] Wang Lin *et al.*, in *Proc. IPAC'10*, pp. 2588-2590.

[2] BAI Zheng-He *et al.*, "Lattice optimization for the HLS-Ⅱ storage ring", *Chin. Phys. C (HEP & NP)*, vol.37, no. 1, pp. 017001, 2013.

[3] BAI Zheng-He *et al.*, "Lattice study for the HLS-II storage ring", *Chin. Phys. C (HEP & NP)*, vol.37, no. 4, pp. 047004, 2013.

[4] Y. Wu *et al.*, in *Proc. PAC'01*, pp. 459-461.

[5] A.Terebilo, "Accelerator Toolbox for MATLAB", SLAC-PUB-8732, 2001.

[6] Kennedy, J., Eberhart, R., in *Proc. IJCNN'95*, pp. 1942-1948

[7] Shi, Y., Eberhart, R.C., in *Proc. EP'98*, pp. 69-73.

[8] Z. Bai, L. Wang, W. Li, in *Proc. IPAC'11*, pp. 2271-2273.

[9] Z. Bai, L. Wang, W. Li, in *Proc. IPAC'11*, pp. 948-950.

[10] Gang-Wen Liu *et al.*, "Improved step-by-step chromaticity compensation method for chromatic sextupole optimization", *Chin. Phys. C (HEP & NP)*, vol.40, no. 5, pp. 057002, 2016.

[11] M. Clerc, J. Kennedy, "The particle swarm - explosion, stability, and convergence in a multidimensional complex space", *IEEE Transactions on Evolutionary Computation*, vol. 6, pp: 58~73, 2002.

ISBN 978-3-95450-147-2